NYU WIRELESS TR 2016-002

Technical Report

5G Millimeter-Wave Channel Model Alliance Measurement Parameter, Scenario Parameter, and Measured Path Loss Data List

Hangsong Yan, George R. MacCartney Jr., Shu Sun, and Theodore S. Rappaport

{hy942,gmac,ss7152,tsr}@nyu.edu

NYU WIRELESS
NYU Tandon School of Engineering
2 MetroTech Center, 9th Floor
Brooklyn, NY 11201

September, 2016

Acknowledgment

This work was supported by the NYU WIRELESS Industrial Affiliates Program, and three National Science Foundation (NSF) Research Grants: 1320472, 1302336, and 1555332.

Executive Summary

In this document, detailed information for five millimeter-wave (mmWave) measurement campaigns is provided. The 28 GHz and 73 GHz outdoor measurement campaigns conducted at New York University (NYU) are described in Sections I and II, respectively, and the 38 GHz and 60 GHz outdoor measurement campaigns conducted at the University of Texas at Austin (UTA) are presented in Sections III and IV, respectively [3]-[7], [11]-[19], [30], [33], [34]. The last section (Section V) describes the 28 GHz and 73 GHz indoor measurement campaign conducted at NYU [2], [20], [21]. Each section consists of three subsections, namely, the measurement parameter list, measurement environment description, and measurement results. The measured path loss data and map coordinates are also provided.

Contents

Contents ..... **IV**

List of Figures ..... **V**

List of Tables ..... **VI**

Introduction **1**

Section I: 28 GHz Outdoor Cellular Measurement Campaign [1], [4], [11], [12], [22] **2**

1.1 Measurement Parameter List **2**

1.2 Measurement Environment Description **4**

1.3 Measurement Results **5**

Section II: 73 GHz Outdoor Cellular Measurement Campaign [1], [3], [4], [22] **8**

2.1 Measurement Parameter List **8**

2.2 Measurement Environment Description **10**

2.3 Measurement Results **11**

Section III: 38 GHz Outdoor Cellular and Peer-to-Peer (P2P) Measurement Campaign [1], [4], [6], [11], [22] **14**

3.1 Measurement Parameter List **14**

3.2 Measurement Environment Description **16**

a) Base Station-to-Mobile Scenario 16

b) Peer-to-Peer Scenario 17

3.3 Measurement Results **18**

Section IV: 60 GHz Outdoor P2P and Vehicular Measurement Campaign [1], [4], [6], [7], [22] **20**

4.1 Measurement Parameter List **20**

4.2 Measurement Environment Description **22**

a) Peer-to-Peer Scenario 22

b) Vehicular scenario 22

4.3 Measurement Results **23**

Section V: 28, 73 GHz Indoor Measurement Campaign [2], [20], [21], [22] **24**

5.1 Measurement Parameter List **24**

5.2 Measurement Environment Description **26**

5.3 Measurement Results **28**

List of Figures

Figure 1 Map of TX and RX locations around NYU's Manhattan campus for 28 GHz measurements during the summer of 2012. Yellow starts indicate TX locations and red dots indicate RX locations. 4
Figure 2 Map of TX and RX locations around NYU's Manhattan campus for 73 GHz measurements during the summer of 2013. Yellow stars indicate TX locations and red dots indicate RX locations. 10
Figure 3 Map of the northeastern corner of the University of Texas at Austin campus showing the transmitter and receiver locations. All receiver locations were measured using a narrowbeam 25 dBi gain antenna. About half of the receiver locations were also measured using a wider beam 13.3 dBi antenna. 16
Figure 4 Overhead image of 38 GHz and 60 GHz peer-to-peer measurement area with transmitter location marked as TX and the surrounding receiver locations. 17
Figure 5 Photo of campus measurement location with surrounding buildings, trees, light posts, and handrails. Metallic objects were found to be useful reflectors that can be exploited in non-LOS conditions (circled in photo). 17
Figure 6 Top view of the vehicle measurement set-up. The receiver was placed inside the vehicle at each of the two locations shown, where non-LOS paths were identified by rotating the receiver antenna. Passengers were seated at the front and right rear passenger seats shown by the circles in the bottom diagram during all measurements. 22
Figure 7 Map of the 2 MetroTech Center 9th floor with five TX locations and 33 RX locations. The yellow stars represent the TX locations and the red dots represent the RX locations. The compass in the top right corner indicates the coordinate system used inside the building for AOD and AOA angle conventions and for post-processing analyses. The RX121 and RX161 locations were identical to the RX12 and RX16 locations, however the glass door near RX16 was propped open for RX121 and RX161 measurements, and was closed for RX12 and RX16 measurements. The RX121 and RX161 locations are included in the 48 TX-RX measured locations. 26
Figure 8 TX1 location with surrounding cubicles, desks, chairs, drywall columns, and windows. The TX antenna was placed 2.5 m above the floor, near the 2.7 m tall ceiling. 27

List of Tables

Table 1 TX locations, GPS coordinates in decimal degrees, and TX heights for the 28 GHz measurement campaign in New York City. 4
Table 2 28 GHz TX-RX location combinations with corresponding TX IDs, RX IDs, Latitude (Lat) and Longitude (Long) coordinates in decimal degrees, environment (Env.) type, T-R 3D separation distances in meters, and omnidirectional path loss (PL) values. A "L" means LOS environment whereas a "N" means NLOS environment. A "-" in the path loss value column indicates no signal (i.e. an outage), whereas a "*'' indicates that the location was not considered for omnidirectional path loss. All RX heights were set to 1.5 m AGL. 5
Table 3 TX locations, GPS coordinates in decimal degrees, and TX heights for the 73 GHz measurements. 10
Table 4 73 GHz TX-RX location combinations with corresponding TX IDs, RX IDs, Latitude (Lat) and Longitude (Long) coordinates in decimal degrees, the RX height h_{RX}, where "M" corresponds to a mobile height of 2 m and "B" corresponds to a backhaul height of 4.06 m, environment (Env.) type, T-R 3D separation distances in meters, and omnidirectional path loss (PL) values. A "L" means LOS environment whereas a "N" means NLOS environment. A "-" in the path loss value column indicates no signal (i.e. an outage). 11
Table 5 TX locations and TX heights for the 38 GHz measurements in Austin. 16
Table 6 38 GHz TX-RX location combinations for the narrowbeam cellular measurements with corresponding TX IDs, RX IDs, environment (Env.) type, T-R 3D separation distances in meters, and omnidirectional path loss (PL) values. All RX heights were set to 1.5 m AGL. 18
Table 7 38 GHz TX-RX location combinations for the widebeam cellular measurements with corresponding TX IDs, RX IDs, environment (Env) type, T-R 3D separation distances in meters, and omnidirectional path loss (PL) values. All RX heights were set as 1.5 m AGL. 19
Table 8 38 GHz P2P close-in free space reference distance (d_0 = 1 m) directional path loss model. PLE is the path loss exponent, σ is the standard derivation of the zero-mean Gaussian random variable (shadow factor) about the minimum mean square error (MMSE) line..... 19
Table 9 60 GHz P2P and vehicular close-in free space reference distance (d_0 = 1 m) directional path loss models. PLE is the path loss exponent, σ is the standard deviation of the zero-mean Gaussian random variable (shadow factor) about the MMSE line. 23
Table 10 28 GHz co-polarized antenna (V-V) omnidirectional path loss values with corresponding Environment (Env.), TX IDs, RX IDs, path loss (PL) in dB, and 3D T-R separation distance in meters. 28
Table 11 28 GHz cross-polarized antenna (V-H) omnidirectional path loss values with corresponding Environment (Env.), TX IDs, RX IDs, path loss (PL) in dB, and 3D T-R separation distance in meters. 29
Table 12 73 GHz co-polarized antenna (V-V) omnidirectional path loss values with corresponding Environment (Env.), TX IDs, RX IDs, path loss (PL) in dB, and 3D T-R separation distance in meters. 30
Table 13 73 GHz cross-polarized antenna (V-H) omnidirectional path loss values with corresponding Environment (Env.), TX IDs, RX IDs, path loss (PL) in dB, and 3D T-R separation distance in meters. 31

Introduction

As annual mobile traffic will continue growing at extremely fast rates [43], [44], [45], current wireless spectrum (below 6 GHz) will not meet future demand. A very promising method to solve this problem is to use the spectrum above 6 GHz and up to 300 GHz (higher centimeter-wave and millimeter-wave bands) due to the vast spectrum bandwidth available at these frequencies. This report presents five extensive millimeter-wave (mmWave) measurement campaigns which were conducted from 2011 to 2014 at New York University (NYU) and University of Texas at Austin (UTA) [2], [3]-[7], [11]-[19], [21], [33], [34]. A wideband sliding correlator channel sounder with directive rotatable horn antennas at both the transmitter (TX) and receiver (RX) were used for all the measurement campaigns. The mmWave frequencies considered in these measurement campaigns include 28 GHz, 38 GHz, 60 GHz and 73 GHz. Apart from diverse frequency bands measured, a broad range of measurement scenarios were also included: base station-to-mobile, base station-to-backhaul, peer-to-peer (P2P) and in-vehicle scenarios. For each measurement campaign, detailed information of the measurement parameters, measurement environment, and measurement results is provided.

These measurement campaigns provided in this report will aid researchers in channel characterization and modeling [13], [15], [30], [32], [34], the design of ray tracers [35], [36], [37], [38], [39], [48]-[51] signal transmission simulator [40], [41], [42], and the construction of beamforming and beam combining techniques [16], [19] for future fifth-generation (5G) mmWave systems. In order to facilitate easy comparisons and improvements between different propagation and channel model results, the path loss parameters for all the measurement campaigns provided in the report are based on a 1 m close-in free space reference distance path loss model [1], [4], [30].

In this report, Section I presents the 28 GHz outdoor cellular measurement campaign in an urban microcell (UMi) environment. The 73 GHz outdoor cellular measurement campaign described in Section II was also measured in a UMi environment, but two scenarios were considered, which were base station-to-backhaul and base station-to-mobile scenarios. Section III describes the 38 GHz outdoor measurement campaign consisted of base station-to-mobile and P2P scenarios. It is worth mentioning that the 38 GHz cellular measurements were conducted in both UMi and urban macrocell (UMa) environments since different TX antenna heights were used in this scenario. The 60 GHz outdoor measurement campaign is presented in Section IV where detailed information of P2P and vehicular scenarios included in this measurement is provided. The last section (Section V) presents an indoor measurement campaign including two frequency bands which are 28 GHz and 73 GHz. The journal papers that most represent the findings of this report are [1], [2],and [4].

Section I: 28 GHz Outdoor Cellular Measurement Campaign [1], [4], [11], [12], [22]

1.1 Measurement Parameter List [4], [11], [12], [22]

Parameter	Parameter description
Basic channel sounder architecture	
Transmit signal	Sinusoid/VNA, binary pseudo random signal, chirp, FMCW, OFDM
	Pseudorandom binary sequence (PRBS) was transmitted.
Signal recording	Real-time sampling, periodic subsampling, sliding correlation (bandwidth compression), frequency sweep
	Signal was recorded by sliding correlation (bandwidth compression) [11], [22]-[27].
Tx Antenna architecture	omni vs directive, single vs array
	Single directive rotatable horn antenna.
Rx Antenna architecture	Omni vs directive, single vs array
	Single directive rotatable horn antenna.
Antenna array architecture	One sided vs. two sided, parallel vs. switched antenna access vs. synthetic aperture. Same for TX and RX?
	Single rotatable horn antenna at both TX and RX.
Tx/Rx synchronization	Cable or fiber synchronization, atomic/GPS clock remote synchronization
	Frequency was synchronized, phase was not synchronized (free running high-stability oscillator at both Tx and Rx, frequency tuning was performed at the beginning of each day).
Dual Polarization capability	Number of parallel Tx/Rx channels (1x1, 2x1, 1x2, 2x2), true parallel or switched? HP/VP or LHCP/RHCP)
	Number of parallel Tx/Rx channels was: 1×1, Tx and Rx antennas were both vertically polarized (VP/VP).
Auxiliary remarks	Rotatable pyramidal horn antenna with gain 24.5 dBi, AZ. HPBW 10.9° and EL. HPBW 8.6° was used at both transmitter and receiver [1], [4], [11], [12], [13], [16], [18], [19], [33], [34].
Key technical parameters	
Center Frequency	28.0 GHz [4], [11], [12]
Bandwidth and spectrum envelope shape/filter	rectangular, sinc^2, etc.
	The first null-to-null RF bandwidth was 800 MHz and the spectrum envelope shape was sinc^2 [1], [4], [11], [13], [16], [18], [34].
CIR period	Alternative: difference between frequency samples(=1/CIR period)
	5117.5 ns undilated, 40.9 ms dilated (slide factor of 8000) [4], [11], [13], [18], [19], [34].
Tx power	Power at input port of antenna? Radiated power? If radiated power, provide antenna gain. Provide methodology.
	Power at input port of antenna was 30.1 dBm [4], [11], [34].
Maximum instantaneous dynamic range	dB difference in the peak of the power delay profile or received CW signal in the passband for LOS only (just below saturation) and peak noise level, without temporal averaging. Noise level must be defined (e.g., thermal, quantization, correlation noise, etc.)
	The maximum instantaneous dynamic range was 30 dB based on thermal noise and quantization noise (8-bit ADC digitizer).

Measurable channel attenuation range	dB difference between lowest and highest channel attenuation that can be measured with an SNR of xx dB. The AGC range over which the defined instantaneous dynamic range can be maintained.
	Measurable channel attenuation range was 170-180 dB with an SNR of 5 dB. Linear response was guaranteed by using selective attenuator [4], [1], [11], [13], [34].
CIR repetition rate f_{CIR} (Hz)	The inverse of the time between received CIRs. Determines maximum Doppler bandwidth, where BW=1/2 f_{CIR}
	24.45 Hz [4], [11], [18], [34].
Averaging	No. of averages in complex and/or power domain. Time alignment method?
	Single power delay profile (PDP) was acquired by averaging 20 consecutive PDP snapshot samples with each sample lasting 40.9 ms [4], [11], [18], [34]. Time alignment method was based on peak voltage trigger.
Auxiliary remarks	Additional details of this measurement campaign can be found in [1], [4], [11]-[13], [15], [16], [18], [19], [33], [34].
Calibration procedures	
Frequency response	Back to back? Including antennas? Bandwidth, number of frequency points, number of power levels. Including AGC?
	Antennas were included.
Received power/path loss	Wideband? Narrowband? Number of power levels checked? Antennas included? If so, how is antenna gain determined?
	Both wideband and narrowband were used in calibration procedures. The calibration attenuation setting at the receiver was from 0 dB to 70 dB with 10 dB increments for each step. The received power/path loss was calculated with antenna gain removed. Antenna gain was determined by the "three antenna method" [29] and verified by antenna specification sheet. The gain of converter box is flat across the 800 MHz frequency bandwidth [32]. Free space path loss calibration was conducted using a 5 meter close-in free space power measurement [11], [12], [18].
Antennas and antenna arrays	Complex radiation patterns? Including polarization? Including azimuth and elevation (full solid angle)? Including antenna switch and feeds?
	Single rotatable horn antenna was used at both Tx and Rx. The antenna polarization configuration used in the calibration was VP/VP (both Tx and Rx antennas vertically polarized). Azimuth and elevation angles were included.
Tx/Rx LO frequency synchronization (in case of remote operation)	Training of atomic clocks
	Frequency was tuned at the beginning of each day and synchronized.
Auxiliary remarks	Additional details of this measurement campaign can be found in [1], [4], [11]-[13], [15], [16], [18], [19], [33], [34].

1.2 Measurement Environment Description [4], [11], [12]

The 28 GHz outdoor measurement campaign was conducted in the summer of 2012 in downtown Manhattan around NYU's main campus which is a dense urban microcell (UMi) environment [4], [11], [12], [18]-[19], [34]. A map describing the specific locations of TX and RX is shown in Figure 1.

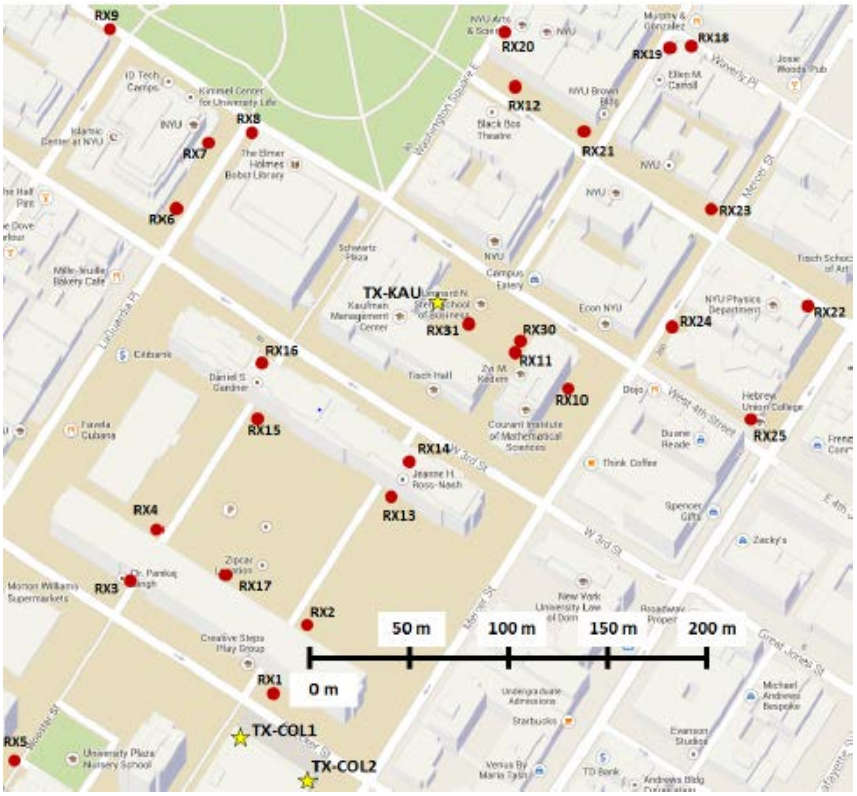

Figure 1 Map of TX and RX locations around NYU's Manhattan campus for 28 GHz measurements during the summer of 2012. Yellow starts indicate TX locations and red dots indicate RX locations [1].

According to Figure 1, three TX locations and 27 RX locations were included in the 28 GHz outdoor measurement campaign, and six line-of-sight (LOS) and 68 non-line-of-sight (NLOS) TX-RX location combinations were measured [1], [4], [11]. Signal was detected at all the LOS and 20 NLOS locations [1], [4], [31]. All of the RX antennas were set at 1.5 m above ground level (AGL) around typical sidewalks on the NYU campus [3]. The heights and the specific GPS coordinates of TX antennas are provided in Table 1.

Table 1 TX locations, GPS coordinates in decimal degrees, and TX heights for the 28 GHz measurement campaign in New York City [3].

TX ID	Latitude (°)	Longitude (°)	Height (m)
COL1	40.7270944	-73.9974972	7
COL2	40.7268833	-73.9970556	7
KAU	40.7290611	-73.9962500	17

The overall environment of this outdoor measurement campaign was a typical urban microcell environment which mainly consisted of NYU's school buildings, apartment complex (Washington Square Village), foliage, lamp-posts, vehicles, signs and handrails. Almost all of the buildings surrounding NYU's main campus had 7-12 stories except for the apartment

complex located in the southwest part of Figure 1. The apartment complex contained two parallel tower slabs of two buildings each and each building had around 16 stories. As seen from Figure 1, one tower slab was exactly in front of TX-COL1 and part in front of TX-COL2.

COL1 and COL2 were located on the northwest and northeast corners of the Coles Sports Center rooftop, respectively [4]. It should be noted that the rooftop of Coles Sports Center was a tennis court, and on the left side of COL1 the foliage was very dense. On the other side, in front of COL2 was a relatively open area but the foliage with around 5 m away was also very dense. TX location KAU was placed on the fifth-story balcony of the Kaufman Business School [4], [11]. This TX location was surrounded by NYU's school buildings which were around 10 stories. The foliage around this TX location was sparse. Additional details about the environment of this measurement campaign can be found in [1], [4], [11]. Table 2 shows the measurement path loss results for 28 GHz outdoor measurement campaign where GPS coordinates, environment type, TX-RX 3D separation distance and omnidirectional path loss value for each TX-RX location combination are provided.

1.3 Measurement Results [1]

Table 2 28 GHz TX-RX location combinations with corresponding TX IDs, RX IDs, Latitude (Lat) and Longitude (Long) coordinates in decimal degrees, environment (Env.) type, T-R 3D separation distances in meters, and omnidirectional path loss (PL) values. A "L" means LOS environment whereas a "N" means NLOS environment. A "-" in the path loss value column indicates no signal (i.e. an outage), whereas a "*'' indicates that the location was not considered for omnidirectional path loss. All RX heights were set to 1.5 m AGL [1].

TX	RX	Lat (°)	Long (°)	Env.	3D T-R (m)	PL (dB)
COL1	1	40.7273222	-73.9973000	L	31	92.3
COL1	2	40.7275417	-73.9970833	N	61	123.8
COL1	3	40.7279056	-73.9980556	L	102	*
COL1	4	40.7280750	-73.9980167	N	118	136.4
COL1	5	40.7269861	-73.9988417	N	114	115.6
COL1	6	40.7295000	-73.9978889	N	270	-
COL1	7	40.7298361	-73.9976167	N	305	-
COL1	8	40.7297444	-73.9971278	N	296	-
COL1	9	40.7303444	-73.9983000	N	368	-
COL1	10	40.7286694	-73.9955139	N	242	-
COL1	11	40.7287806	-73.9957667	N	238	-
COL1	12	40.7300500	-73.9957083	N	362	-
COL1	13	40.7281139	-73.9966750	N	133	132.9
COL1	14	40.7283472	-73.9964389	N	165	137.1
COL1	15	40.7285319	-73.9973250	N	159	-
COL1	16	40.7287500	-73.9973000	N	185	-
COL1	17	40.7278333	-73.9975000	N	82	148.1
COL1	18	40.7301222	-73.9945389	N	419	-
COL1	19	40.7302361	-73.9948806	N	413	-
COL1	20	40.7302833	-73.9958972	N	379	-
COL1	21	40.7299306	-73.9954500	N	360	-
COL1	22	40.7290528	-73.9940278	N	365	-

COL1	23	40.7295556	-73.9946806	N	362	-
COL1	24	40.7289722	-73.9948361	N	306	-
COL1	25	40.7285361	-73.9943917	N	307	-
COL2	1	40.7273222	-73.9973000	L	53	100.8
COL2	2	40.7275417	-73.9970833	N	73	121.4
COL2	3	40.7279056	-73.9980556	N	142	119
COL2	4	40.7280750	-73.9980167	N	155	141.4
COL2	5	40.7269861	-73.9988417	N	151	124.9
COL2	6	40.7295000	-73.9978889	N	299	-
COL2	7	40.7298361	-73.9976167	N	332	-
COL2	8	40.7297444	-73.9971278	N	318	-
COL2	9	40.7303444	-73.9983000	N	399	-
COL2	10	40.7286694	-73.9955139	N	237	-
COL2	11	40.7287806	-73.9957667	N	237	-
COL2	12	40.7300500	-73.9957083	N	370	-
COL2	13	40.7281139	-73.9966750	N	141	124.8
COL2	14	40.7283472	-73.9964389	N	171	144.5
COL2	15	40.7285139	-73.9973250	N	183	-
COL2	16	40.7287500	-73.9973000	N	209	-
COL2	17	40.7278333	-73.9975000	N	112	142.2
COL2	18	40.7301222	-73.9945389	N	418	-
COL2	19	40.7302361	-73.9948806	N	415	-
COL2	20	40.7302833	-73.9958972	N	390	-
COL2	21	40.7299306	-73.9954500	N	365	-
COL2	22	40.7290528	-73.9940278	N	351	-
COL2	23	40.7295556	-73.9946806	N	358	-
COL2	24	40.7289722	-73.9948361	N	298	-
COL2	25	40.7285361	-73.9943917	N	290	-
KAU	1	40.7273222	-73.9973000	N	213	-
KAU	2	40.7275417	-73.9970833	N	184	-
KAU	3	40.7279056	-73.9980556	N	200	-
KAU	4	40.7280750	-73.9980167	N	186	149.2
KAU	5	40.7269861	-73.9988417	N	318	-
KAU	6	40.7295000	-73.9978889	N	147	-
KAU	7	40.7298361	-73.9976167	N	145	-
KAU	8	40.7297444	-73.9971278	N	107	-
KAU	9	40.7303444	-73.9983000	N	225	-
KAU	10	40.7286694	-73.9955139	N	77	124.2
KAU	11	40.7287806	-73.9957667	L	54	102.1
KAU	12	40.7300500	-73.9957083	N	120	140
KAU	13	40.7281139	-73.9966750	N	112	-

KAU	14	40.7283472	-73.9964389	N	82	127
KAU	15	40.7285139	-73.9973250	N	110	-
KAU	16	40.7287500	-73.9973000	N	96	140
KAU	17	40.7278333	-73.9975000	N	173	-
KAU	18	40.7301222	-73.9945389	N	187	-
KAU	19	40.7302361	-73.9948806	N	175	137
KAU	20	40.7302833	-73.9958972	N	140	-
KAU	21	40.7299306	-73.9954500	N	119	118
KAU	22	40.7290528	-73.9940278	N	188	-
KAU	30	40.7287806	-73.9957667	L	53	94.6
KAU	31	40.7288778	-73.9960028	L	33	88.4

Section II: 73 GHz Outdoor Cellular Measurement Campaign [1], [3], [4], [22]

2.1 Measurement Parameter List [3], [4], [22]

Parameter	Parameter description
Basic channel sounder architecture	
Transmit signal	Sinusoid/VNA, binary pseudo random signal, chirp, FMCW, OFDM
	Pseudorandom binary sequence (PRBS) was transmitted.
Signal recording	Real-time sampling, periodic subsampling, sliding correlation (bandwidth compression), frequency sweep
	Signal was recorded by sliding correlation (bandwidth compression) [11], [22]-[27].
Tx Antenna architecture	omni vs directive, single vs array
	Single directive rotatable horn antenna.
Rx Antenna architecture	Omni vs directive, single vs array
	Single directive rotatable horn antenna.
Antenna array architecture	One sided vs. two sided, parallel vs. switched antenna access vs. synthetic aperture. Same for TX and RX?
	Single rotatable horn antenna at both TX and RX.
Tx/Rx synchronization	Cable or fiber synchronization, atomic/GPS clock remote synchronization
	Frequency was synchronized, phase was not synchronized (free running high-stability oscillator at both Tx and Rx, frequency tuning was performed at the beginning of each day).
Dual Polarization capability	Number of parallel Tx/Rx channels (1x1, 2x1, 1x2, 2x2), true parallel or switched? HP/VP or LHCP/RHCP)
	Number of parallel Tx/Rx channels was: 1×1, both transmitter and receiver antennas were vertically polarized (VP/VP).
Auxiliary remarks	Rotatable pyramidal horn antenna with gain 27 dBi, AZ. HPBW 7° and EL. HPBW 7° was used at both transmitter and receiver [1], [3], [4], [34].
Key technical parameters	
Center Frequency	73.5 GHz [3], [4]
Bandwidth and spectrum envelope shape/filter	rectangular, sinc^2, etc.
	The first null-to-null RF bandwidth was 800 MHz and the spectrum envelope shape was sinc^2 [3], [4], [34].
CIR period	Alternative: difference between frequency samples(=1/CIR period)
	5117.5 ns undilated, 40.9 ms dilated (slide factor of 8000) [3], [4], [16], [34].
Tx power	Power at input port of antenna? Radiated power? If radiated power, provide antenna gain. Provide methodology.
	Power at input port of antenna was 14.6 dBm [3], [4], [34].
Maximum instantaneous dynamic range	dB difference in the peak of the power delay profile or received CW signal in the passband for LOS only (just below saturation) and peak noise level, without temporal averaging. Noise level must be defined (e.g., thermal, quantization, correlation noise, etc.)
	The maximum instantaneous dynamic range was 30 dB based on thermal noise and quantization noise (8-bit ADC digitizer).
	dB difference between lowest and highest channel attenuation that can be measured with an SNR of xx dB. The AGC range over

Measurable channel attenuation range	which the defined instantaneous dynamic range can be maintained.
	Measurable channel attenuation range was 170-180 dB with an SNR of 5 dB. Linear response was guaranteed by using selective attenuator [3], [4], [15], [34].
CIR repetition rate f_{CIR} (Hz)	The inverse of the time between received CIRs. Determines maximum Doppler bandwidth, where BW=1/2 f_{CIR}
	24.45 Hz [3], [4], [16], [34].
Averaging	No. of averages in complex and/or power domain. Time alignment method?
	Single PDP was acquired by averaging 20 consecutive PDP snapshot samples with each sample lasting 40.9 ms [3], [4], [16], [34]. Time alignment method was based on peak voltage trigger.
Auxiliary remarks	Additional details of this measurement campaign can be found in [1], [3], [4], [15], [16], [34].
Calibration procedures	
Frequency response	Back to back? Including antennas? Bandwidth, number of frequency points, number of power levels. Including AGC?
	Antennas were included.
Received power/path loss	Wideband? Narrowband? Number of power levels checked? Antennas included? If so, how is antenna gain determined?
	Both wideband and narrowband were used in calibration procedures. The calibration attenuation setting at the receiver was from 0 dB to 70 dB with 10 dB increments for each step. The received power/path loss was calculated with antenna gain removed. The antenna gain was determined by the ”three antenna method” [29] and verified by antenna specification sheet. The gain of converter box is flat across the 800 MHz frequency bandwidth [32]. Free space path loss calibration was conducted using a 4 meter close-in free space power measurement [3], [16].
Antennas and antenna arrays	Complex radiation patterns? Including polarization? Including azimuth and elevation (full solid angle)? Including antenna switch and feeds?
	Single rotatable horn antenna was used at both Tx and Rx. The antenna polarization configuration used in the calibration was VP/VP (both Tx and Rx antennas were vertically polarized). Azimuth and elevation angles were included.
Tx/Rx LO frequency synchronization (in case of remote operation)	Training of atomic clocks
	Frequency was tuned at the beginning of each day and synchronized.
Auxiliary remarks	Additional details of this measurement campaign can be found in [1], [3], [4], [15], [16], [34].

2.2 Measurement Environment Description [3], [4]

The 73 GHz outdoor measurement campaign was conducted in the summer of 2013 in downtown Manhattan around NYU's main campus which is a dense UMi environment [3], [4], [15]-[16], [34]. A map describing the specific locations of TX and RX is shown in Figure 2.

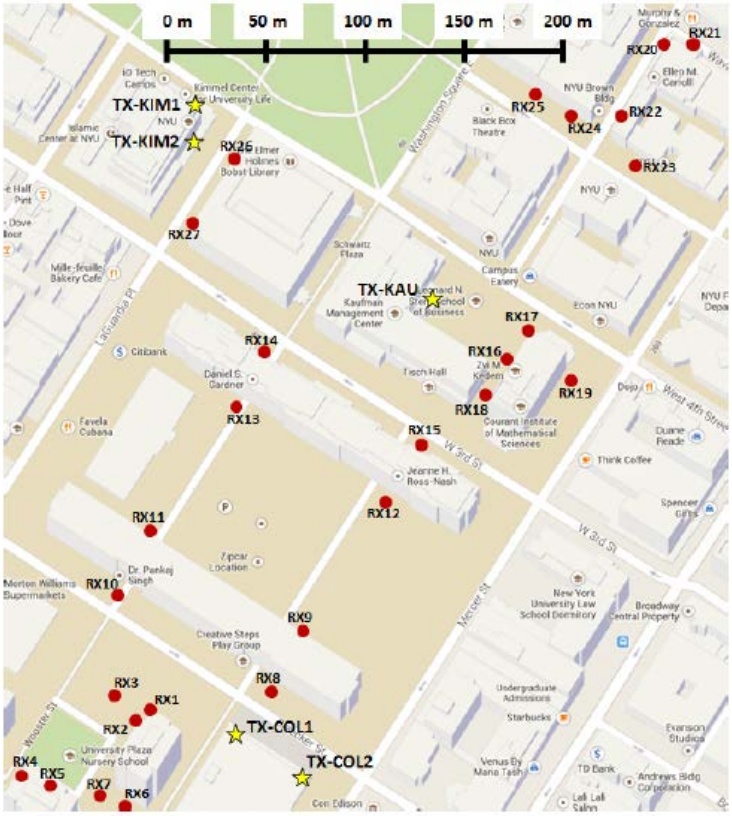

Figure 2 Map of TX and RX locations around NYU's Manhattan campus for 73 GHz measurements during the summer of 2013. Yellow stars indicate TX locations and red dots indicate RX locations [3].

In the 73 GHz outdoor measurement campaign, two more TX locations were considered besides KAU, COL1, and COL2, and their GPS coordinates and antenna heights are provided in Table 3.

Table 3 TX locations, GPS coordinates in decimal degrees, and TX heights for the 73 GHz measurements [3].

TX ID	Latitude (°)	Longitude (°)	Height (m)
COL1	40.7270944	-73.9974972	7
COL2	40.7268833	-73.9970556	7
KAU	40.7290611	-73.9962500	17
KIM1	40.7300472	-73.9978333	7
KIM2	40.7297444	-73.9977222	7

The extra two TX locations KIM1 and KIM2 were situated on the northwest and southeast corners of the 2nd-floor balcony of the Kimmel center of NYU [4]. On the right side of KIM1 and KIM2 was the Elmer Holmes Bobst Library which was a 12-story, 425,000 square feet (39,500 m^2) structure [8]. In front of KIM1 and KIM2 was the Washington Square Park which had dense foliage and may affect the signals transmitted from KIM1 and KIM2, and received by the RXs located in the northeast corner of Figure 2. Additional details about the environment of this measurement campaign can be found in [1], [3], [4].

The number of RX locations for this measurement campaign was also 27, but there were two kinds of RX antenna height scenarios; the mobile scenario had RX antenna heights of 2 m AGL and the backhaul scenario had RX antenna heights of 4.06 m AGL [3], [4]. There were 36 and 38 TX-RX location combinations measured for mobile and backhaul scenarios, respectively [1], [4], [31]. Signal was detected at 30 TX-RX locations for mobile scenarios which include all the five LOS locations and 25 NLOS locations. On the other hand, for the backhaul scenario (five LOS and 34 NLOS locations), signal was detected at all the LOS locations and 28 NLOS locations [4], [31]. The measurement results for 73 GHz outdoor measurement campaign is shown in Table 4 where GPS coordinates, environment type, TX-RX 3D separation, RX antenna height, and path loss value for each TX-RX location combination is provided.

2.3 Measurement Results [1]

Table 4 73 GHz TX-RX location combinations with corresponding TX IDs, RX IDs, Latitude (Lat) and Longitude (Long) coordinates in decimal degrees, the RX height h_{RX}, where "M" corresponds to a mobile height of 2 m and "B" corresponds to a backhaul height of 4.06 m, environment (Env.) type, T-R 3D separation distances in meters, and omnidirectional path loss (PL) values. A "L" means LOS environment whereas a "N" means NLOS environment. A "-" in the path loss value column indicates no signal (i.e. an outage) [1].

TX	RX	Lat (°)	Long (°)	h_{RX}	Env.	3D T-R (m)	PL (dB)
COL1	1	40.7270861	-73.9980611	M	N	48	123.7
COL1	2	40.7270361	-73.9981167	M	N	53	136.5
COL1	3	40.7271917	-73.9982417	M	N	64	128.2
COL1	4	40.7269000	-73.9987000	M	N	104	131.8
COL1	5	40.7268472	-73.9985722	M	N	95	132.3
COL1	6	40.7267694	-73.9982250	M	N	71	136.2
COL1	7	40.7268111	-73.9983194	M	N	76	136.7
COL1	8	40.7272972	-73.9972694	M	L	30	108.4
COL1	9	40.7275139	-73.9970806	B	N	58	137.4
COL1	10	40.7277861	-73.9981556	B	N	95	137.3
COL1	11	40.7279917	-73.9980242	B	N	109	150.9
COL1	12	40.7281306	-73.9965472	B	N	140	138.3
COL1	13	40.7286333	-73.9975111	M	N	171	-
COL1	13	40.7286333	-73.9975111	B	N	171	-
COL1	14	40.7288139	-73.9973361	M	N	192	-
COL1	14	40.7288139	-73.9973361	B	N	192	-
COL1	15	40.7283639	-73.9964111	M	N	168	-
COL1	15	40.7283639	-73.9964111	B	N	168	-
COL2	1	40.7270861	-73.9980611	B	N	88	132.2
COL2	2	40.7270361	-73.9981167	M	N	91	140.7
COL2	2	40.7270361	-73.9981167	B	N	91	143
COL2	3	40.7271917	-73.9982417	M	N	106	137.6
COL2	3	40.7271917	-73.9982417	B	N	106	137.3
COL2	4	40.7269000	-73.9987000	M	N	139	148.1
COL2	4	40.7269000	-73.9987000	B	N	139	154.6
COL2	5	40.7268472	-73.9985722	M	N	128	148.2

COL2	5	40.7268472	-73.9985722	B	N	128	147.9
COL2	6	40.7267694	-73.9982250	M	N	99	158
COL2	6	40.7267694	-73.9982250	B	N	99	144.3
COL2	7	40.7268111	-73.9983194	B	N	107	148.6
COL2	8	40.7272972	-73.9972694	M	L	50	108.1
COL2	9	40.7275139	-73.9970806	B	N	70	142.1
COL2	10	40.7277861	-73.9981556	B	N	137	136
COL2	11	40.7279917	-73.9980242	B	N	148	159.7
COL2	12	40.7281306	-73.9965472	B	N	145	139.8
COL2	13	40.7286333	-73.9975111	M	N	198	-
COL2	13	40.7286333	-73.9975111	B	N	198	-
COL2	14	40.7288139	-73.9973361	M	N	216	-
COL2	14	40.7288139	-73.9973361	B	N	216	-
COL2	15	40.7283639	-73.9964111	M	N	173	-
COL2	15	40.7283639	-73.9964111	B	N	173	-
KAU	15	40.7283639	-73.9964111	M	N	80	134.6
KAU	15	40.7283639	-73.9964111	B	N	80	139.5
KAU	16	40.7287639	-73.9957806	M	L	54	99.5
KAU	16	40.7287639	-73.9957806	B	L	54	99.4
KAU	17	40.7289361	-73.9957167	M	L	49	103.3
KAU	17	40.7289361	-73.9957167	B	L	49	106.1
KAU	18	40.7285917	-73.9959694	M	N	59	117.4
KAU	18	40.7285917	-73.9959694	B	N	59	122.9
KAU	19	40.7287472	-73.9954278	M	N	79	128
KAU	19	40.7287472	-73.9954278	B	N	79	135.5
KAU	20	40.7301583	-73.9948972	M	N	168	136.1
KAU	20	40.7301583	-73.9948972	B	N	168	145.9
KAU	21	40.7301833	-73.9947111	M	N	181	133.5
KAU	21	40.7301833	-73.9947111	B	N	181	137.4
KAU	22	40.7298583	-73.9951444	M	N	129	129.2
KAU	22	40.7298583	-73.9951444	B	N	129	139.6
KAU	23	40.7296889	-73.9950056	M	N	127	135.1
KAU	23	40.7296889	-73.9950056	B	N	127	140.4
KAU	24	40.7299028	-73.9954194	M	N	118	133.6
KAU	24	40.7299028	-73.9954194	B	N	118	118.6
KAU	25	40.7299694	-73.9955833	M	N	117	138.3
KAU	25	40.7299694	-73.9955833	B	N	117	133.3
KIM1	25	40.7299694	-73.9955833	M	N	190	146
KIM1	25	40.7299694	-73.9955833	B	N	190	149.3
KIM1	26	40.7297389	-73.9974000	M	N	50	132
KIM1	26	40.7297389	-73.9974000	B	N	50	133.3

KIM1	27	40.7293861	-73.9976972	M	N	74	135
KIM1	27	40.7293861	-73.9976972	B	N	74	137.3
KIM2	25	40.7299694	-73.9955833	M	N	182	154.5
KIM2	25	40.7299694	-73.9955833	B	N	182	156.2
KIM2	26	40.7297389	-73.9974000	B	L	27	103.3
KIM2	27	40.7293861	-73.9976972	M	L	40	98
KIM2	27	40.7293861	-73.9976972	B	L	40	97.8

Section III: 38 GHz Outdoor Cellular and Peer-to-Peer (P2P) Measurement Campaign [1], [4], [6], [11], [22]

3.1 Measurement Parameter List [4], [6], [11], [22]

Parameter	Parameter description
Basic channel sounder architecture	
Transmit signal	Sinusoid/VNA, binary pseudo random signal, chirp, FMCW, OFDM
	Pseudorandom binary sequence (PRBS) was transmitted.
Signal recording	Real-time sampling, periodic subsampling, sliding correlation (bandwidth compression), frequency sweep
	Signal was recorded by sliding correlation (bandwidth compression) [11], [22]-[27].
Tx Antenna architecture	omni vs directive, single vs array
	Single directive rotatable horn antenna.
Rx Antenna architecture	Omni vs directive, single vs array
	Single directive rotatable horn antenna.
Antenna array architecture	One sided vs. two sided, parallel vs. switched antenna access vs. synthetic aperture. Same for TX and RX?
	Single rotatable horn antenna at both TX and RX.
Tx/Rx synchronization	Cable or fiber synchronization, atomic/GPS clock remote synchronization
	Frequency was synchronized, phase was not synchronized (free running high-stability oscillator at both Tx and Rx, frequency tuning was performed at the beginning of each day).
Dual Polarization capability	Number of parallel Tx/Rx channels (1x1, 2x1, 1x2, 2x2), true parallel or switched? HP/VP or LHCP/RHCP)
	Number of parallel Tx/Rx channels was: 1×1, both TX and RX antennas were vertically polarized (VP/VP).
Auxiliary remarks	Identical Ka-band vertically polarized rotatable horn antennas were used at transmitter and receiver. For TX locations, narrowbeam antennas with gain 25 dBi, AZ. HPBW 7.8° were used. For RX locations, both narrowbeam antenna (gain 25 dBi, AZ. HPBW 7.8°) and widebeam antenna (gain 13.3 dBi, AZ. HPBW 49.4°) were used [1], [4], [5], [6], [11], [13], [14], [47].
Key technical parameters	
Center Frequency	37.625 GHz [4], [5], [6], [11], [14], [47]
Bandwidth and spectrum envelope shape/filter	rectangular, sinc^2, etc.
	The first null-to-null RF bandwidth was 800 MHz and the spectrum envelope shape was sinc^2 [1], [4], [5], [11], [13].
CIR period	Alternative: difference between frequency samples(=1/CIR period)
	5117.5 ns undilated, 40.9 ms dilated (slide factor of 8000) [4], [6], [11], [13], [14].
Tx power	Power at input port of antenna? Radiated power? If radiated power, provide antenna gain. Provide methodology.
	Power at input port of antenna was 21.2 dBm [1], [4], [6], [14].
Maximum instantaneous dynamic range	dB difference in the peak of the power delay profile or received CW signal in the passband for LOS only (just below saturation) and peak noise level, without temporal averaging. Noise level must be defined (e.g., thermal, quantization, correlation noise, etc.)

	The maximum instantaneous dynamic range was 30 dB based on thermal noise and quantization noise.
Measurable channel attenuation range	dB difference between lowest and highest channel attenuation that can be measured with an SNR of xx dB. The AGC range over which the defined instantaneous dynamic range can be maintained.
	Measurable channel attenuation range was 150-160 dB. Linear response was guaranteed by using selective attenuator [1], [4], [6], [11], [13], [14].
CIR repetition rate f_{CIR} (Hz)	The inverse of the time between received CIRs. Determines maximum Doppler bandwidth, where BW=1/2 f_{CIR}
	24.45 Hz [4], [6].
Averaging	No. of averages in complex and/or power domain. Time alignment method?
	Single PDP was acquired by averaging 20 consecutive PDP snapshot samples with each sample lasting 40.9 ms [4], [6]. Time alignment method was based on peak voltage trigger.
Auxiliary remarks	Additional details of this measurement campaign can be found in [1], [4], [5], [6], [11], [13], [14], [46], [47].
Calibration procedures	
Frequency response	Back to back? Including antennas? Bandwidth, number of frequency points, number of power levels. Including AGC?
	Antennas were included.
Received power/path loss	Wideband? Narrowband? Number of power levels checked? Antennas included? If so, how is antenna gain determined?
	Both wideband and narrowband were used in calibration procedures. The calibration attenuation setting at the receiver was from 0 dB to 70 dB with 10 dB increments for each step. The received power/path loss was calculated with antenna gain removed. The antenna gain was determined by the "three antenna method" [29] and verified by antenna specification sheet. The gain of converter box is flat across the 800 MHz frequency bandwidth [32]. Free space path loss calibrations were conducted using 3 and 5 meter close-in free space power measurements for peer-to-peer and base station-to-mobile access scenarios, respectively [6].
Antennas and antenna arrays	Complex radiation patterns? Including polarization? Including azimuth and elevation (full solid angle)? Including antenna switch and feeds?
	Single rotatable horn antenna was used at both Tx and Rx. The antenna polarization configuration used in the calibration was VP/VP (both Tx and Rx antennas vertically polarized). Azimuth and elevation angles were included.
Tx/Rx LO frequency synchronization (in case of remote operation)	Training of atomic clocks
	Frequency was tuned at the beginning of each day and synchronized.
Auxiliary remarks	Additional details of this measurement campaign can be found in [1], [4], [5], [6], [11], [13], [14], [46], [47].

3.2 Measurement Environment Description [4], [6], [11]

The 38 GHz outdoor measurement campaign was conducted in the summer of 2011 at the UTA campus [4], [6], [47], which represents urban macrocell (UMa) and UMi environments. Two scenarios were considered in this measurement campaign which includes *Base Station-to-Mobile Scenario* and *Peer-to-Peer (P2P) Scenario*.

a) Base Station-to-Mobile Scenario

A map describing the TX and RX locations for this scenario is given in Figure 3.

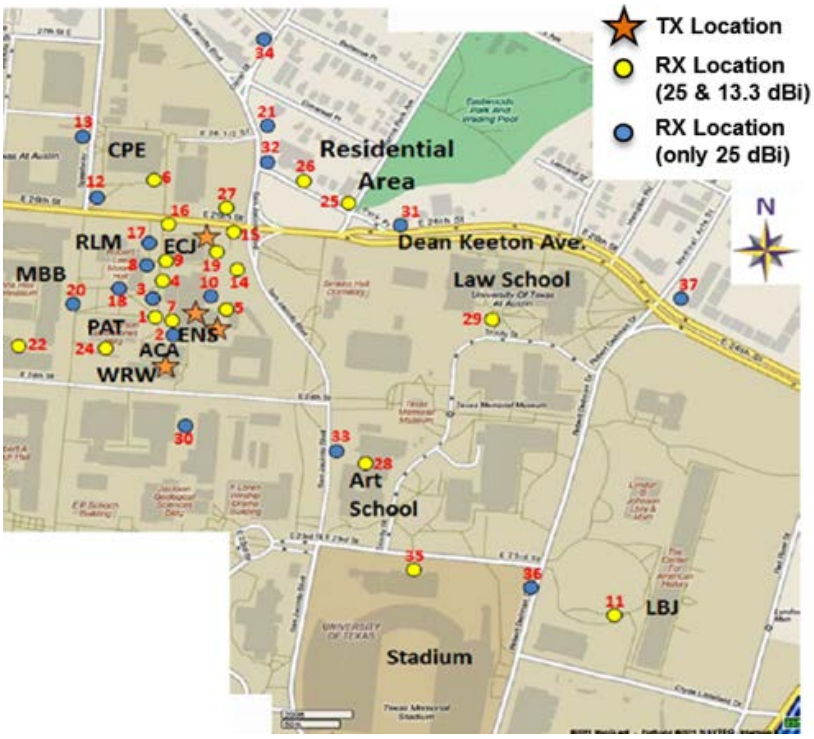

Figure 3 Map of the northeastern corner of the University of Texas at Austin campus showing the transmitter and receiver locations. All receiver locations were measured using a narrowbeam 25 dBi gain antenna. About half of the receiver locations were also measured using a wider beam 13.3 dBi antenna [5].

As shown in Figure 3, four TX locations and 37 RX locations were considered in this measurement campaign [1], [4]. All the RX antenna heights were set as 1.5 m AGL, and the information of TX antenna heights are provided in Table 5. Additional details about the measurement environment of this scenario can be found in [1], [4], [5], [6], [11].

Table 5 TX locations and TX heights for the 38 GHz measurements in Austin [5].

TX ID	Height
ECJ	8
WRW	23
ENSA	36
ENSB	36

Both narrowbeam and widebeam antennas were used for different RX locations in this measurement campaign with 43 and 22 TX-RX location combinations for narrowbeam and widebeam scenarios, respectively [1], [4], [6], [14]. The measurement results for this scenario are presented in Table 6 and Table 7, respectively.

b) Peer-to-Peer Scenario

In this scenario, one TX location and 10 RX locations were selected in a pedestrian walkway courtyard surrounded by many buildings with 6-10 stories on the UTA campus [6]. Little vegetation can be observed in the courtyard but several lamp poles existed [6], [7]. A map describing the TX and RX locations and a photo of the TX site environment for this scenario are shown in Figure 4 and Figure 5, respectively. Both the TX and RX antenna heights were set at 1.5 m AGL representative of people holding mobile devices [7]. Additional details of the measurement environment of this scenario can be found in [1], [4], [6], [7], [11].

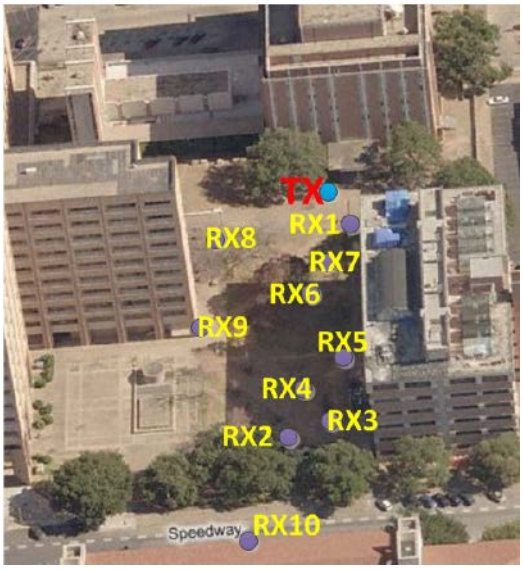

Figure 4 Overhead image of 38 GHz and 60 GHz peer-to-peer measurement area with transmitter location marked as TX and the surrounding receiver locations [6].

Figure 5 Photo of campus measurement location with surrounding buildings, trees, light posts, and handrails. Metallic objects were found to be useful reflectors that can be exploited in non-LOS conditions (circled in photo) [7].

In Table 8 the close-in free space reference distance (d_0 = 1 m) directional path loss model [4] for this scenario are presented.

3.3 Measurement Results [1], [4]

Table 6 38 GHz TX-RX location combinations for the narrowbeam cellular measurements with corresponding TX IDs, RX IDs, environment (Env.) type, T-R 3D separation distances in meters, and omnidirectional path loss (PL) values. All RX heights were set to 1.5 m AGL [1].

TX	RX	Env.	3D T-R (m)	PL (dB)
ECJ	5	L	104	99.6
ECJ	14	L	70	91.3
ECJ	27	L	49	108.0
ECJ	10	N	65	126.5
ECJ	15	N	29	119.6
ECJ	16	N	53	101.1
ECJ	25	N	185	126.8
ECJ	26	N	156	123.4
ECJ	31	N	225	131.7
ECJ	32	N	135	129.3
WRW	1	L	74	98.5
WRW	3	L	115	110.1
WRW	4	L	139	107.9
WRW	6	L	265	110.8
WRW	7	L	70	100.2
WRW	8	L	163	106.5
WRW	22	L	203	108.4
WRW	2	N	61	111.4
WRW	18	N	145	113.2
WRW	20	N	150	139.0
WRW	24	N	101	119.7
ENSA	6	L	200	108.5
ENSA	9	L	122	106.9
ENSA	12	L	200	104.4
ENSA	14	L	85	105.1
ENSA	19	L	110	98.9
ENSA	21	L	291	103.1
ENSA	11	L	728	115.0
ENSA	21	L	295	114.2
ENSB	30	L	132	98.5
ENSB	33	L	245	107.8
ENSB	34	L	410	113.5
ENSB	35	L	448	117.6
ENSB	36	L	570	116.6
ENSB	37	L	930	121.6
ENSA	4	N	75	117.4
ENSA	13	N	295	142.3
ENSA	17	N	118	126.6
ENSA	20	N	159	134.0
ENSA	25	N	270	115.7

ENSB	28	N	284	118.4
ENSB	29	N	377	115.3
ENSB	31	N	282	127.7

Table 7 38 GHz TX-RX location combinations for the widebeam cellular measurements with corresponding TX IDs, RX IDs, environment (Env) type, T-R 3D separation distances in meters, and omnidirectional path loss (PL) values. All RX heights were set as 1.5 m AGL [1].

TX	RX	Env.	3D T-R (m)	PL (dB)
ECJ	5	L	104	99.3
ECJ	14	L	70	98.0
ECJ	27	L	50	104.1
ECJ	15	N	29	112.9
ECJ	16	N	54	98.9
ECJ	26	N	156	123.7
WRW	1	L	74	100.6
WRW	4	L	139	102.2
WRW	6	L	265	104.4
WRW	7	L	70	95.8
WRW	22	L	203	108.4
WRW	24	N	101	116.4
ENSA	6	L	200	104.5
ENSA	9	L	122	101.6
ENSA	19	L	110	101.6
ENSB	11	L	728	113.6
ENSB	35	L	448	115.1
ENSA	4	N	75	112.7
ENSA	25	N	270	115.2
ENSB	11	N	728	129.4
ENSB	28	N	284	115.8
ENSB	29	N	377	117.5

Table 8 38 GHz P2P close-in free space reference distance (d_0 = 1 m) directional path loss model. PLE is the path loss exponent, σ is the standard derivation of the zero-mean Gaussian random variable (shadow factor) about the minimum mean square error (MMSE) line [4].

38 GHz P2P Directional Path Loss Models (d_0 = 1 m)								
			LOS		NLOS		NLOS-best	
Frequency	TX Height (m)	RX Height (m)	PLE	σ [dB]	PLE	σ [dB]	PLE	σ [dB]
38 GHz	1.5	1.5	2.0	3.8	3.9	10.6	3.3	7.7

Section IV: 60 GHz Outdoor P2P and Vehicular Measurement Campaign [1], [4], [6], [7], [22]

4.1 Measurement Parameter List [4], [6], [7], [22]

Parameter	Parameter description
Basic channel sounder architecture	
Transmit signal	Sinusoid/VNA, binary pseudo random signal, chirp, FMCW, OFDM
	Pseudorandom binary sequence (PRBS) was transmitted.
Signal recording	Real-time sampling, periodic subsampling, sliding correlation (bandwidth compression), frequency sweep
	Signal was recorded by sliding correlation (bandwidth compression) [11], [22]-[27]
Tx Antenna architecture	omni vs directive, single vs array
	Single directive rotatable horn antenna.
Rx Antenna architecture	Omni vs directive, single vs array
	Single directive rotatable horn antenna.
Antenna array architecture	One sided vs. two sided, parallel vs. switched antenna access vs. synthetic aperture. Same for TX and RX?
	Single rotatable horn antenna at TX and RX.
Tx/Rx synchronization	Cable or fiber synchronization, atomic/GPS clock remote synchronization
	Frequency was synchronized, phase was not synchronized (free running high-stability oscillator at both Tx and Rx, frequency tuning was performed at the beginning of each day).
Dual Polarization capability	Number of parallel Tx/Rx channels (1x1, 2x1, 1x2, 2x2), true parallel or switched? HP/VP or LHCP/RHCP)
	Number of parallel Tx/Rx channels was: 1×1, both Tx and Rx antennas were vertically polarized (VP/VP).
Auxiliary remarks	Identical U-band vertically polarized rotatable horn antennas with gains of 25 dBi and beamwidth of 7.3° were used at the transmitter and receiver [4], [6], [7].
Key technical parameters	
Center Frequency	59.4 GHz [4], [6]
Bandwidth and spectrum envelope shape/filter	rectangular, sinc^2, etc.
	The first null-to-null RF bandwidth was 1.5 GHz and spectrum envelope shape was sinc^2 [4], [7].
CIR period	Alternative: difference between frequency samples(=1/CIR period)
	2729.3 ns undilated, 54.6 ms dilated (slide factor of 20000) [4], [6], [7].
Tx power	Power at input port of antenna? Radiated power? If radiated power, provide antenna gain. Provide methodology.
	Power at input port of antenna was 5 dBm [4], [6], [7].
Maximum instantaneous dynamic range	dB difference in the peak of the power delay profile or received CW signal in the passband for LOS only (just below saturation) and peak noise level, without temporal averaging. Noise level must be defined (e.g., thermal, quantization, correlation noise, etc.)
	The maximum instantaneous dynamic range was 30 dB based on thermal noise and quantization noise.
	dB difference between lowest and highest channel attenuation that can be measured with an SNR of xx dB. The AGC range over

Measurable channel attenuation range	which the defined instantaneous dynamic range can be maintained.
	Measurable channel attenuation range was 150-160 dB. Linear response was guaranteed by using selective attenuator [4], [6].
CIR repetition rate f_{CIR} (Hz)	The inverse of the time between received CIRs. Determines maximum Doppler bandwidth, where BW=1/2 f_{CIR}
	18.32 Hz [4], [7].
Averaging	No. of averages in complex and/or power domain. Time alignment method?
	Single PDP was acquired by averaging 20 consecutive PDP snapshot samples with each sample lasting 54.6 ms [4], [7]. Time alignment method was based on peak voltage trigger.
Auxiliary remarks	**Additional details of this measurement campaign can be found in [4], [6], [7].**
Calibration procedures	
Frequency response	Back to back? Including antennas? Bandwidth, number of frequency points, number of power levels. Including AGC?
	Antennas were included.
Received power/path loss	Wideband? Narrowband? Number of power levels checked? Antennas included? If so, how is antenna gain determined?
	Both wideband and narrowband were used in calibration procedures. The calibration attenuation setting at the receiver was from 0 dB to 70 dB with 10 dB increments for each step [7]. The received power/path loss was calculated with antenna gain removed. The antenna gain was determined by the "three antenna method" [29] and verified by antenna specification sheet. The gain of converter box is flat across the 1.5 GHz frequency bandwidth [32]. Free space path loss calibration was conducted using a 3 meter close-in free space power measurement [6].
Antennas and antenna arrays	Complex radiation patterns? Including polarization? Including azimuth and elevation (full solid angle)? Including antenna switch and feeds?
	Single rotatable horn antenna was used at both Tx and Rx. The antenna polarization configuration used in the calibration was VP/VP (both Tx and Rx antennas vertically polarized). Azimuth and elevation angles were included.
Tx/Rx LO frequency synchronization (in case of remote operation)	Training of atomic clocks
	Frequency was tuned at the beginning of each day and synchronized.
Auxiliary remarks	**Additional details of this measurement campaign can be found in [4], [6], [7].**

4.2 Measurement Environment Description [4], [6], [7]

The 60 GHz outdoor measurement campaign was also conducted in the summer of 2011 in the UTA campus [4], [6], [7]. Two scenarios were considered in this measurement campaign which includes *Peer-to-Peer Scenario* and *Vehicular Scenario*.

a) Peer-to-Peer Scenario

The same TX and RX locations as considered in 38 GHz P2P measurement campaign were selected for 60 GHz P2P measurements and the detailed description of this measurement layout and environment are given in Figure 4 and Figure 5. Additional details about the measurement environment of this scenario can be found in [4], [6], [7].

b) Vehicular scenario

The 60 GHz vehicular scenario measurement was conducted in a parking lot on the UTA campus. The RX antenna was placed at head level of a seated passenger in a standard-sized sedan automobile (2003 Mitsubishi Galant) [7]. Two RX sites were considered in this scenario, which were the driver position and a rear passenger position. A photo of the experimental automobile and the detailed locations of the RX sites are provided in Figure 6.

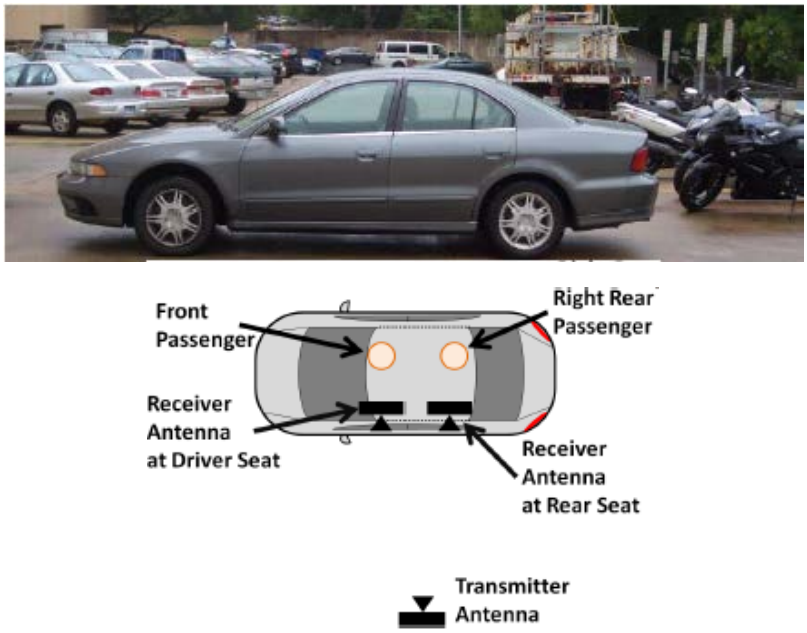

Figure 6 Top view of the vehicle measurement set-up. The receiver was placed inside the vehicle at each of the two locations shown, where non-LOS paths were identified by rotating the receiver antenna. Passengers were seated at the front and right rear passenger seats shown by the circles in the bottom diagram during all measurements [7].

The TX locations were set 4, 12, and 23 m away from the RX location, which represent scenarios of a single lane of traffic, a two-way street, and a multilane highway [4], [28]. The TX antenna height was set as 1.5 m AGL. Additional details about the measurement environment of this scenario can be found in [4], [6], [7]. In Table 9 the 60 GHz P2P and vehicular close-in free space reference distance (d_0 = 1 m) directional path loss models [4] are presented.

4.3 Measurement Results [4]

Table 9 60 GHz P2P and vehicular close-in free space reference distance (d_0 = 1 m) directional path loss models. PLE is the path loss exponent, σ is the standard deviation of the zero-mean Gaussian random variable (shadow factor) about the MMSE line [4].

60 GHz P2P Directional Path Loss Models (d_0 = 1 m)								
			LOS		NLOS		NLOS-best	
Frequency	TX Height (m)	RX Height (m)	PLE	σ [dB]	PLE	σ [dB]	PLE	σ [dB]
60 GHz	1.5	1.5	2.2	2.0	3.6	9.0	3.3	9.2
60 GHz Vehicular Directional Path Loss Models (d_0 = 1 m)								
			LOS		NLOS		NLOS-best	
Frequency	TX Height (m)	RX Height (m)	PLE	σ [dB]	PLE	σ [dB]	PLE	σ [dB]
60 GHz	1.5	1.5	2.5	3.5	5.4	14.8	5.0	10.9

Section V: 28, 73 GHz Indoor Measurement Campaign [2], [20], [21], [22]

5.1 Measurement Parameter List [2], [20], [21], [22]

Parameter	Parameter description
Basic channel sounder architecture	
Transmit signal	Sinusoid/VNA, binary pseudo random signal, chirp, FMCW, OFDM
	Pseudorandom binary sequence (PRBS) was transmitted.
Signal recording	Real-time sampling, periodic subsampling, sliding correlation (bandwidth compression), frequency sweep
	Signal was recorded by sliding correlation (bandwidth compression) [11], [22]-[27].
Tx Antenna architecture	omni vs directive, single vs array
	Single directive rotatable horn antenna.
Rx Antenna architecture	Omni vs directive, single vs array
	Single directive rotatable horn antenna.
Antenna array architecture	One sided vs. two sided, parallel vs. switched antenna access vs. synthetic aperture. Same for TX and RX?
	Single rotatable horn antenna at both TX and RX.
Tx/Rx synchronization	Cable or fiber synchronization, atomic/GPS clock remote synchronization
	Frequency was synchronized, phase was not synchronized (free running high-stability oscillator at both Tx and Rx, frequency tuning was performed at the beginning of each day).
Dual Polarization capability	Number of parallel Tx/Rx channels (1x1, 2x1, 1x2, 2x2), true parallel or switched? HP/VP or LHCP/RHCP)
	Number of parallel Tx/Rx channels was: 1×1, Tx antenna was vertically polarized and Rx antenna had two polarized configurations (vertical and horizontal polarizations).
Auxiliary remarks	Mechanically rotatable directional horn antenna with gain 15 dBi, AZ. HPBW 28.8°, EL. HPBW 30° was used at the transmitter and receiver for 28 GHz. For 73 GHz, mechanically rotatable directional horn antenna with gain 20 dBi, AZ. HPBW 15° and EL. HPBW 15° was used at the transmitter and receiver [2], [21].
Key technical parameters	
Center Frequency	28.0 GHz, 73.5 GHz [2], [21]
Bandwidth and spectrum envelope shape/filter	rectangular, sinc^2, etc.
	The first null-to-null RF bandwidth was 800 MHz and spectrum envelope shape was sinc^2 [2], [21].
CIR period	Alternative: difference between frequency samples(=1/CIR period)
	5117.5 ns undilated, 40.9 ms dilated (slide factor of 8000) [2], [21].
Tx power	Power at input port of antenna? Radiated power? If radiated power, provide antenna gain. Provide methodology.
	Power at input port of antenna were 23.9 dBm for 28 GHz and 12.1 dBm for 73 GHz [2], [21].
Maximum instantaneous dynamic range	dB difference in the peak of the power delay profile or received CW signal in the passband for LOS only (just below saturation) and peak noise level, without temporal averaging. Noise level must be defined (e.g., thermal, quantization, correlation noise, etc.)

	The maximum instantaneous dynamic range was 30 dB based on thermal noise and quantization noise (8-bit ADC digitizer).
Measurable channel attenuation range	dB difference between lowest and highest channel attenuation that can be measured with an SNR of xx dB. The AGC range over which the defined instantaneous dynamic range can be maintained.
	Measurable channel attenuation range was 150-160 dB with an SNR of 5 dB. Linear response was guaranteed by using selective attenuator [2], [21].
CIR repetition rate f_{CIR} (Hz)	The inverse of the time between received CIRs. Determines maximum Doppler bandwidth, where BW=1/2 f_{CIR}
	24.45 Hz [2], [21].
Averaging	No. of averages in complex and/or power domain. Time alignment method?
	Single PDP was acquired by averaging 20 consecutive PDP snapshot samples with each sample lasting 40.9 ms [2], [21]. Time alignment method was based on peak voltage trigger.
Auxiliary remarks	Additional details of this measurement campaign can be found in [2], [20], [21].
Calibration procedures	
Frequency response	Back to back? Including antennas? Bandwidth, number of frequency points, number of power levels. Including AGC?
	Antennas were included.
Received power/path loss	Wideband? Narrowband? Number of power levels checked? Antennas included? If so, how is antenna gain determined?
	Both wideband and narrowband were used in calibration procedures. The calibration attenuation setting at the receiver was from 0 dB to 70 dB with 10 dB increments for each step. The received power/path loss was calculated with antenna gain removed. The antenna gain was determined by the "three antenna method" [29] and verified by antenna specification sheet. The gain of converter box is flat across the 800 MHz frequency bandwidth [32]. Free space path loss calibration was conducted using a 4 meter close-in free space power measurement [2], [21].
Antennas and antenna arrays	Complex radiation patterns? Including polarization? Including azimuth and elevation (full solid angle)? Including antenna switch and feeds?
	Single rotatable horn antenna was used at both Tx and Rx. The antenna polarization configuration used in the calibration was VP/VP (both Tx and Rx antennas vertically polarized). Azimuth and elevation angles were included.
Tx/Rx LO frequency synchronization (in case of remote operation)	Training of atomic clocks
	Frequency was tuned at the beginning of each day and synchronized.
Auxiliary remarks	Additional details of this measurement campaign can be found in [2], [20], [21].

5.2 Measurement Environment Description [2], [20], [21]

The 28 and 73 GHz indoor measurement campaign was conducted in the summer of 2014 in the NYU WIRELESS research center which is on the 9th floor of 2 MetroTech Center in downtown Brooklyn, New York [2], [20], [21]. A map describing the indoor measurement environment and the specific TX and RX locations is shown in Figure 7.

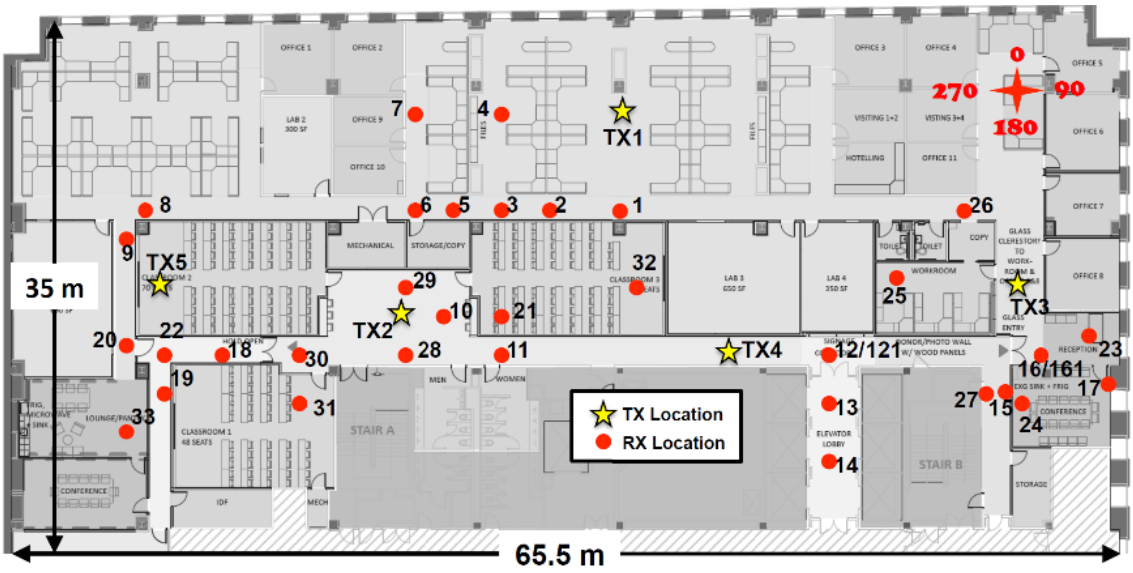

Figure 7 Map of the 2 MetroTech Center 9th floor with five TX locations and 33 RX locations. The yellow stars represent the TX locations and the red dots represent the RX locations. The compass in the top right corner indicates the coordinate system used inside the building for AOD and AOA angle conventions and for post-processing analyses. The RX121 and RX161 locations were identical to the RX12 and RX16 locations, however the glass door near RX16 was propped open for RX121 and RX161 measurements, and was closed for RX12 and RX16 measurements. The RX121 and RX161 locations are included in the 48 TX-RX measured locations [2].

2 MetroTech Center in downtown Brooklyn, New York is a 10-story building constructed in the early 1990's with tinted windows and steel reinforcement between each floor [2]. NYU WIRELESS research center on the 9th floor is a typical single-floor office environment with common obstructions: desks, chairs, cubicle partitions, offices, classrooms, doors, hallways, walls made of drywall, and elevators.

Five TX and 33 RX locations were considered in this indoor measurement campaign with total 48 TX-RX location combinations for both 28 and 73 GHz. The 48 location combinations consisted of 10 LOS and 38 NLOS measurement scenarios and can be mainly divided into 3 kinds of environment which are defined below [2]:

Corridor Environment: a propagating signal travels down a corridor to reach the receiver by a LOS path, reflections, scattering, and/or diffraction, but not penetration.

Open-plan environment: a cubicle-farm and a central TX location around soft partitions such as cubicle walls [9], [10].

Closed-plan environment: a propagating signal must penetrate an obstruction such as a fixed building wall to reach the receiver.

All the TX antenna heights in this measurement campaign are set as 2.5 m AGL which is close to the 2.7 m ceiling and all the RX antenna heights are set as 1.5 m AGL which is the typical handset level height [2].

Figure 8 shows the surrounding environment of TX1 where some obstructions in this

environment are denoted.

Figure 8 TX1 location with surrounding cubicles, desks, chairs, drywall columns, and windows. The TX antenna was placed 2.5 m above the floor, near the 2.7 m tall ceiling [2].

According to Figure 7, we can see that RX4 and 7 had similar surrounding environment as TX1. The difference between RX7 and TX1 was that the western side of RX7 was the offices of NYU WIRELESS faculties, which consisted of drywalls and windows.

TX2 was set at a rest area on the 9th floor. This rest area was surrounded by drywalls and had a corridor in the southern side. It can be observed that RX10 and 29 had similar environment as TX2.

TX3 was set in the hallway of NYU WIRELESS research center. The eastern and western sides of TX3 were drywalls with windows mounted.

The surrounding environment of TX4 was a typical corridor with drywalls on the northern and southern sides. Similar to TX4, RX11, 30, 18, 19, 9, 20, 13, 14, 15, 27, and 26 were also in a corridor environment. In addition, RX 1, 2, 3, 5, 6, and 8 can also be seen in a corridor environment but their northern side was an office region with environment similar to the one shown in Figure 8.

TX5 was set in the front of a typical classroom with surrounding drywalls and several rows of desks and chairs in the middle. It is easy to observe from Figure 7 that RX21, 32 and 31 were also set in a classroom. Moreover, RX17 and 24 were set in a conference room which had similar environment as TX5. Additional details about the environment of this measurement campaign can be found in [2], [20], [21].

The measurement results for 28 GHz and 73 GHz indoor measurement campaign are presented in Table 10, Table 11, Table 12, and Table 13 where omnidirectional path loss values for co-polarized (V-V) and cross-polarized (V-H) antenna configurations are provided.

5.3 Measurement Results [2]

Table 10 28 GHz co-polarized antenna (V-V) omnidirectional path loss values with corresponding Environment (Env.), TX IDs, RX IDs, path loss (PL) in dB, and 3D T-R separation distance in meters [2].

28 GHz Omnidirectional V-V Path Loss				
Env.	TX ID	RX ID	PL (dB)	3D T-R (m)
LOS	1	1	69.3	6.4
LOS	1	4	75.3	7.9
LOS	1	7	76.5	12.9
LOS	2	10	66.3	4.1
LOS	3	16	68.0	5.3
LOS	4	11	74.3	12.7
LOS	4	12	70.4	7.1
LOS	4	28	75.4	21.3
LOS	4	121	71.3	7.1
LOS	4	161	74.5	20.6
NLOS	1	2	76.6	7.8
NLOS	1	3	82.7	10.1
NLOS	1	5	84.3	11.9
NLOS	1	6	86.4	14.4
NLOS	1	8	95.9	25.9
NLOS	1	9	118.5	32.9
NLOS	2	11	78.5	9.0
NLOS	2	12	89.5	28.5
NLOS	2	13	113.1	29.2
NLOS	2	14	119.3	30.4
NLOS	2	15	115.8	39.2
NLOS	2	16	97.8	41.9
NLOS	2	17	120.5	45.9
NLOS	2	18	93.6	12.1
NLOS	2	19	103.1	15.5
NLOS	2	20	111.3	17.1
NLOS	2	21	78.0	6.7
NLOS	2	22	95.3	14.8
NLOS	2	161	98.6	41.9
NLOS	3	17	85.8	8.7
NLOS	3	23	79.9	5.6
NLOS	3	24	86.1	7.8
NLOS	3	25	76.31	8.4
NLOS	3	26	72.9	5.5
NLOS	3	27	75.8	8.3
NLOS	4	13	97.2	8.2
NLOS	4	14	105.0	10.8
NLOS	4	15	97.5	20.8
NLOS	4	16	80.0	20.6
NLOS	4	18	96.8	33.0

NLOS	5	8	73.8	3.9
NLOS	5	19	75.3	6.9
NLOS	5	28	86.1	15.6
NLOS	5	29	81.3	15.0
NLOS	5	30	88.7	11.4
NLOS	5	31	90.4	13.9
NLOS	5	32	90.2	31.2
NLOS	5	33	97.0	9.1

Table 11 28 GHz cross-polarized antenna (V-H) omnidirectional path loss values with corresponding Environment (Env.), TX IDs, RX IDs, path loss (PL) in dB, and 3D T-R separation distance in meters [2].

28 GHz Omnidirectional V-H Path Loss				
Env.	TX ID	RX ID	PL (dB)	3D T-R (m)
LOS	1	1	84.1	6.4
LOS	1	4	87.7	7.9
LOS	1	7	89.7	12.9
LOS	2	10	78.6	4.1
LOS	3	16	83.4	5.3
LOS	4	11	88.2	12.7
LOS	4	12	85.1	7.1
LOS	4	28	90.2	21.3
LOS	4	121	85.0	7.1
LOS	4	161	89.8	20.6
NLOS	1	2	88.2	7.8
NLOS	1	3	91.3	10.1
NLOS	1	5	94.7	11.9
NLOS	1	6	100.1	14.4
NLOS	1	8	115.3	25.9
NLOS	2	11	88.5	9.0
NLOS	2	12	108.8	28.5
NLOS	2	13	141.6	29.2
NLOS	2	14	139.6	30.4
NLOS	2	16	113.4	41.9
NLOS	2	18	98.9	12.1
NLOS	2	19	113.7	15.5
NLOS	2	20	120.4	17.1
NLOS	2	21	83.7	6.7
NLOS	2	22	101.6	14.8
NLOS	2	161	110.5	41.9
NLOS	3	17	97.2	8.7
NLOS	3	23	92.7	5.6
NLOS	3	24	95.8	7.8
NLOS	3	25	88.9	8.4
NLOS	3	26	86.7	5.5

NLOS	3	27	89.3	8.3
NLOS	4	13	104.6	8.2
NLOS	4	14	112.8	10.8
NLOS	4	15	108.4	20.8
NLOS	4	16	93.7	20.6
NLOS	4	18	109.4	33.0
NLOS	5	8	89.3	3.9
NLOS	5	19	91.5	6.9
NLOS	5	28	98.4	15.6
NLOS	5	29	93.7	15.0
NLOS	5	30	96.1	11.4
NLOS	5	31	100.2	13.9
NLOS	5	32	104.8	31.2
NLOS	5	33	104.6	9.1

Table 12 73 GHz co-polarized antenna (V-V) omnidirectional path loss values with corresponding Environment (Env.), TX IDs, RX IDs, path loss (PL) in dB, and 3D T-R separation distance in meters [2].

73 GHz Omnidirectional V-V Path Loss				
Env.	TX ID	RX ID	PL (dB)	3D T-R (m)
LOS	1	1	81.7	6.4
LOS	1	4	81.2	7.9
LOS	1	7	86.7	12.9
LOS	2	10	79.9	4.1
LOS	3	16	82.4	5.3
LOS	4	11	84.1	12.7
LOS	4	12	82.3	7.1
LOS	4	28	82.6	21.3
LOS	4	121	83.2	7.1
LOS	4	161	84.6	20.6
NLOS	1	2	92.1	7.8
NLOS	1	3	89.8	10.1
NLOS	1	5	100.4	11.9
NLOS	1	6	104.0	14.4
NLOS	1	8	121.8	25.9
NLOS	2	11	92.8	9.0
NLOS	2	12	102.1	28.5
NLOS	2	13	118.9	29.2
NLOS	2	14	127.4	30.4
NLOS	2	15	142.5	39.2
NLOS	2	16	111.2	41.9
NLOS	2	18	115.7	12.1
NLOS	2	19	142.5	15.5
NLOS	2	21	94.5	6.7
NLOS	2	22	116.3	14.8

NLOS	2	161	108.2	41.9
NLOS	3	17	107.5	8.7
NLOS	3	23	102.7	5.6
NLOS	3	24	111.4	7.8
NLOS	3	25	90.4	8.4
NLOS	3	26	93.3	5.5
NLOS	3	27	89.7	8.3
NLOS	4	13	104.7	8.2
NLOS	4	14	115.5	10.8
NLOS	4	15	114.2	20.8
NLOS	4	16	102.4	20.6
NLOS	4	18	108.4	33.0
NLOS	5	8	91.0	3.9
NLOS	5	19	90.2	6.9
NLOS	5	28	100.1	15.6
NLOS	5	29	94.7	15.0
NLOS	5	30	107.6	11.4
NLOS	5	31	112.8	13.9
NLOS	5	32	105.5	31.2
NLOS	5	33	118.7	9.1

Table 13 73 GHz cross-polarized antenna (V-H) omnidirectional path loss values with corresponding Environment (Env.), TX IDs, RX IDs, path loss (PL) in dB, and 3D T-R separation distance in meters [2].

73 GHz Omnidirectional V-H Path Loss				
Env.	TX ID	RX ID	PL (dB)	3D T-R (m)
LOS	1	1	102.4	6.4
LOS	1	4	100.4	7.9
LOS	1	7	111.5	12.9
LOS	2	10	101.3	4.1
LOS	3	16	102.9	5.3
LOS	4	11	108.2	12.7
LOS	4	12	104.0	7.1
LOS	4	28	106.6	21.3
LOS	4	121	106.0	7.1
LOS	4	161	108.7	20.6
NLOS	1	2	106.1	7.8
NLOS	1	3	108.8	10.1
NLOS	1	5	116.7	11.9
NLOS	1	6	115.3	14.4
NLOS	2	11	110.6	9
NLOS	2	12	124.2	28.5
NLOS	2	16	138.9	41.9
NLOS	2	18	130.6	12.1
NLOS	2	21	111.0	6.7

NLOS	2	22	126.6	14.8
NLOS	2	161	126.4	41.9
NLOS	3	17	122.3	8.7
NLOS	3	23	117.2	5.6
NLOS	3	24	122.1	7.8
NLOS	3	25	109.7	8.4
NLOS	3	26	104.8	5.5
NLOS	3	27	113.3	8.3
NLOS	4	13	123.4	8.2
NLOS	4	14	140.2	10.8
NLOS	4	15	134.2	20.8
NLOS	4	16	116.2	20.6
NLOS	4	18	129.9	33.0
NLOS	5	8	106.7	3.9
NLOS	5	19	112.8	6.9
NLOS	5	28	117.7	15.6
NLOS	5	29	117.4	15.0
NLOS	5	30	125.8	11.4
NLOS	5	31	120.2	13.9
NLOS	5	32	128.3	31.2
NLOS	5	33	132.1	9.1

References

[1] G. R. MacCartney, T. S. Rappaport, M. K. Samimi and S. Sun, "Millimeter-Wave Omnidirectional Path Loss Data for Small Cell 5G Channel Modeling," in *IEEE Access*, vol. 3, pp. 1573-1580, 2015.

[2] G. R. MacCartney, T. S. Rappaport, S. Sun and S. Deng, "Indoor Office Wideband Millimeter-Wave Propagation Measurements and Channel Models at 28 and 73 GHz for Ultra-Dense 5G Wireless Networks," in *IEEE Access*, vol. 3, pp. 2388-2424, 2015.

[3] G. R. MacCartney and T. S. Rappaport, "73 GHz millimeter wave propagation measurements for outdoor urban mobile and backhaul communications in New York City," *2014 IEEE International Conference on Communications (ICC)*, Sydney, NSW, 2014, pp. 4862-4867.

[4] T. S. Rappaport, G. R. MacCartney, M. K. Samimi and S. Sun, "Wideband Millimeter-Wave Propagation Measurements and Channel Models for Future Wireless Communication System Design," in *IEEE Transactions on Communications*, vol. 63, no. 9, pp. 3029-3056, Sept. 2015.

[5] T. S. Rappaport, F. Gutierrez, E. Ben-Dor, J. N. Murdock, Y. Qiao and J. I. Tamir, "Broadband Millimeter-Wave Propagation Measurements and Models Using Adaptive-Beam Antennas for Outdoor Urban Cellular Communications," in *IEEE Transactions on Antennas and Propagation*, vol. 61, no. 4, pp. 1850-1859, April 2013.

[6] T. S. Rappaport, E. Ben-Dor, J. N. Murdock and Y. Qiao, "38 GHz and 60 GHz angle-dependent propagation for cellular & peer-to-peer wireless communications," *2012 IEEE International Conference on Communications (ICC)*, Ottawa, ON, 2012, pp. 4568-4573.

[7] E. Ben-Dor, T. S. Rappaport, Y. Qiao and S. J. Lauffenburger, "Millimeter-Wave 60 GHz Outdoor and Vehicle AOA Propagation Measurements Using a Broadband Channel Sounder," 2011 IEEE *Global Telecommunications Conference (GLOBECOM 2011)*, Houston, TX, USA, 2011, pp. 1-6.

[8] https://en.wikipedia.org/wiki/Elmer_Holmes_Bobst_Library

[9] S. Y. Seidel and T. S. Rappaport, "Path loss prediction in multifloored buildings at 914 MHz," in *Electronics Letters*, vol. 27, no. 15, pp. 1384-1387, 18 July 1991.

[10] S. Y. Seidel and T. S. Rappaport, "914 MHz path loss prediction models for indoor wireless communications in multifloored buildings," in *IEEE Transactions on Antennas and Propagation*, vol. 40, no. 2, pp. 207-217, Feb 1992.

[11] T. S. Rappaport *et al*., "Millimeter Wave Mobile Communications for 5G Cellular: It Will Work!" in IEEE Access, vol. 1, pp. 335-349, 2013.

[12] Y. Azar *et al*., "28 GHz propagation measurements for outdoor cellular communications using steerable beam antennas in New York city," *2013 IEEE International Conference on Communications (ICC)*, Budapest, 2013, pp. 5143-5147.

[13] G. R. MacCartney, Junhong Zhang, Shuai Nie and T. S. Rappaport, "Path loss models for 5G millimeter wave propagation channels in urban microcells," *2013 IEEE Global Communications Conference (GLOBECOM)*, Atlanta, GA, 2013, pp. 3948-3953.

[14] T. S. Rappaport, Y. Qiao, J. I. Tamir, J. N. Murdock and E. Ben-Dor, "Cellular broadband millimeter wave propagation and angle of arrival for adaptive beam steering systems (invited paper)," *2012 IEEE Radio and Wireless Symposium (RWS)*, Santa Clara, CA, 2012, pp. 151-154.

[15] M. R. Akdeniz *et al*., "Millimeter Wave Channel Modeling and Cellular Capacity Evaluation," in *IEEE Journal on Selected Areas in Communications*, vol. 32, no. 6, pp. 1164-1179, June 2014.

[16] S. Sun, G. R. MacCartney, M. K. Samimi, S. Nie and T. S. Rappaport, "Millimeter multi-beam antenna combining for 5G cellular link improvement in New York City,"

2014 IEEE International Conference on Communications (ICC), Sydney, NSW, 2014, pp. 5468-5473.
[17] F. Gutierrez Jr., T. S. Rappaport and J. Murdock, "Millimeter-Wave CMOS Antennas and RFIC Parameter Extraction for Vehicular Applications," in *Proc. IEEE 72nd VTC Fall*, Sep. 2010, pp. 1-6.
[18] M. Samimi *et al*., "28 GHz Angle of Arrival and Angle of Departure Analysis for Outdoor Cellular Communications Using Steerable Beam Antennas in New York City," in *Proc. IEEE 77th VTC-Spring*, Jun. 2013, pp. 1-6.
[19] S. Sun and T. S. Rappaport, "Multi-beam antenna combining for 28 GHz cellular link improvement in urban environments," *2013 IEEE Global Communications Conference (GLOBECOM)*, Atlanta, GA, 2013, pp. 3754-3759.
[20] S. Nie, G. R. MacCartney, S. Sun and T. S. Rappaport, "72 GHz millimeter wave indoor measurements for wireless and backhaul communications," *2013 IEEE 24th Annual International Symposium on Personal, Indoor, and Mobile Radio Communications (PIMRC)*, London, 2013, pp. 2429-2433.
[21] S. Deng, M. K. Samimi and T. S. Rappaport, "28 GHz and 73 GHz millimeter-wave indoor propagation measurements and path loss models," *2015 IEEE International Conference on Communication Workshop (ICCW)*, London, 2015, pp. 1244-1250.
[22] T. S. Rappaport, Wireless communications: principles and practice. 2nd ed. Upper Saddle River, NJ, UAS: Prentice-Hall, 2002.
[23] D. Cox, "Delay Doppler characteristics of multipath propagation at 910 MHz in a suburban mobile radio environment," in *IEEE Transactions on Antennas and Propagation*, vol. 20, no. 5, pp. 625-635, Sep 1972.
[24] G. Martin, "Wideband channel sounding dynamic range using a sliding correlator," in *Proc. IEEE 51st VTC-Spring*, Tokyo, Japan, 2000, vol. 3, pp. 2517-2521.
[25] R. J. Pirkl and G. D. Durgin, "Optimal Sliding Correlator Channel Sounder Design," in *IEEE Transactions on Wireless Communications*, vol. 7, no. 9, pp. 3488-3497, September 2008.
[26] A. Ghosh *et al*., "Millimeter-Wave Enhanced Local Area Systems: A High-Data-Rate Approach for Future Wireless Networks," in *IEEE Journal on Selected Areas in Communications*, vol. 32, no. 6, pp. 1152-1163, June 2014.
[27] T. S. Rappaport, R. W. Heath, Jr., R. C. Daniels, and J. N. Murdock, Millimeter wave wireless communications. Englewood Cliffs, NJ, USA: Prentice Hall, 2015.
[28] T. S. Rappaport, S. DiPierro and R. Akturan, "Analysis and Simulation of Interference to Vehicle-Equipped Digital Receivers From Cellular Mobile Terminals Operating in Adjacent Frequencies," in *IEEE Transactions on Vehicular Technology*, vol. 60, no. 4, pp. 1664-1676, May 2011.
[29] W. H. Kummer, and E. S. Gillespie. "Antenna measurements 1978." *IEEE Proceedings*. Vol. 66. 1978.
[30] S. Sun *et al*., "Investigation of Prediction Accuracy, Sensitivity, and Parameter Stability of Large-Scale Propagation Path Loss Models for 5G Wireless Communications," in *IEEE Transactions on Vehicular Technology*, vol. 65, no. 5, pp. 2843-2860, May 2016.
[31] G. R. MacCartney, M. K. Samimi and T. S. Rappaport, "Exploiting directionality for millimeter-wave wireless system improvement," *2015 IEEE International Conference on Communications (ICC)*, London, 2015, pp. 2416-2422.
[32] M. K. Samimi, "Characterization of the 28 GHz Millimeter-Wave Dense Urban Channel for Future 5G Mobile," *Master of Science Dissertation*, May 2014.

[33] H. Zhao *et al*., "28 GHz millimeter wave cellular communication measurements for reflection and penetration loss in and around buildings in New York city," *2013 IEEE International Conference on Communications (ICC)*, Budapest, 2013, pp. 5163-5167.
[34] M. K. Samimi and T. S. Rappaport, "3-D Millimeter-Wave Statistical Channel Model for 5G Wireless System Design," in *IEEE Transactions on Microwave Theory and Techniques*, vol. 64, no. 7, pp. 2207-2225, July 2016.
[35] S. Y. Seidel and T. S. Rappaport, "Site-specific propagation prediction for wireless in-building personal communication system design," in *IEEE Transactions on Vehicular Technology*, vol. 43, no. 4, pp. 879-891, Nov 1994.
[36] G. Durgin, N. Patwari and T. S. Rappaport, "An advanced 3D ray launching method for wireless propagation prediction," *Vehicular Technology Conference, 1997, IEEE 47th*, Phoenix, AZ, 1997, pp. 785-789 vol.2.
[37] S. Y. Seidel and T. S. Rappaport, "A ray tracing technique to predict path loss and delay spread inside buildings," *1992 IEEE Global Telecommunications Conference*, Orlando, FL, 1992, pp. 649-653 vol.2.
[38] K. R. Schaubach, N. J. Davis and T. S. Rappaport, "A ray tracing method for predicting path loss and delay spread in microcellular environments," *Vehicular Technology Conference, 1992, IEEE 42nd*, Denver, CO, 1992, pp. 932-935 vol.2.
[39] C. M. P. Ho and T. S. Rappaport, "Wireless channel prediction in a modern office building using an image-based ray tracing method," *1993 IEEE Global Telecommunications Conference*, Houston, TX, 1993, pp. 1247-1251 vol.2.
[40] T. S. Rappaport and V. Fung, "Simulation of bit error performance of FSK, BPSK, and π/4 DQPSK in flat fading indoor radio channels using a measurement-based channel model," in *IEEE Transactions on Vehicular Technology*, vol. 40, no. 4, pp. 731-740, Nov 1991.
[41] V. Fung, T. S. Rappaport and B. Thoma, "Bit error simulation for π/4 DQPSK mobile radio communications using two-ray and measurement-based impulse response models," in *IEEE Journal on Selected Areas in Communications*, vol. 11, no. 3, pp. 393-405, Apr 1993.
[42] V. Fung and T. S. Rappaport, "Bit-error simulation of π/4 DQPSK in flat and frequency-selective fading mobile radio channels with real time applications," *1991 IEEE International Conference on Communications*, Denver, pp. 553-557 vol.2.
[43] T. S. Rappaport, "Keynote Speech: Millimeter Wave Wireless Communications-The Renaissance of Computing and Communications," presented at the IEEE International Conference on Communications (ICC), Sydney, Australia, Jun. 2014, slides available at ICC 14 website.
[44] "VNI mobile forecast highlights, 2014–2019," CISCO, San Jose, CA, USA, 2015. Available:http://www.cisco.com/assets/sol/sp/vni/forecast_highlights_mobil/index.html
[45] "Cisco visual networking index: Mobile data traffic forecast update, 2013–2018," CISCO, San Jose, CA, USA, Feb. 2014. [Online]. Available:http://www.cisco.com/c/en /us/solutions /collateral/service-provider/ visual-networking-index-vni/white_paper_c11-520862.pdf
[46] J. N. Murdock, E. Ben-Dor, Y. Qiao, J. I. Tamir and T. S. Rappaport, "A 38 GHz cellular outage study for an urban outdoor campus environment," *2012 IEEE Wireless Communications and Networking Conference (WCNC)*, Shanghai, 2012, pp. 3085-3090.
[47] T. S. Rappaport, Y. Qiao, J. I. Tamir, J. N. Murdock and E. Ben-Dor, "Cellular broadband millimeter wave propagation and angle of arrival for adaptive beam steering systems (invited paper),"*Radio and Wireless Symposium (RWS), 2012 IEEE*, Santa Clara, CA, 2012, pp. 151-154.

[48] G. Durgin, N. Patwari and T. S. Rappaport, "Improved 3D ray launching method for wireless propagation prediction," in *Electronics Letters*, vol. 33, no. 16, pp. 1412-1413, 31 Jul 1997.
[49] K. K. Bae *et al.*, "WCDMA STTD performance analysis with transmitter location optimization in indoor systems using ray-tracing technique," *Radio and Wireless Conference, 2002. RAWCON 2002. IEEE*, 2002, pp. 123-127.
[50] T. T. Tran and T. S. Rappaport, "Site specific propagation prediction models for PCS design and installation," *1992 IEEE Military Communications Conference*, San Diego, CA, 1992, pp. 1062-1065 vol.3.
[51] S. Seidel, K. Schaubach, T. Tran and T. Rappaport, "Research in site-specific propagation modeling for PCS system design," *Vehicular Technology Conference, 1993., 43rd IEEE*, Secaucus, NJ, 1993, pp. 261-264.